

Effect of transmit array phase relationship on local Specific Absorption Rate (SAR)

L. M. Angelone^{1,2}, N. Makris³, C. Vasios², L. Wald², G. Bonmassar²

¹Biomedical Engineering Department, Tufts University, Medford, MA, United States, ²A. Martinos Center for Biomedical Imaging, Massachusetts General Hospital, Charlestown, MA, United States, ³Center for Morphometric Analysis, Massachusetts General Hospital, Charlestown, MA, United States

INTRODUCTION

This study measured the effect of transmit array phase relationship on local Specific Absorption Rate (SAR) to determine if B_1 shimming could yield significantly different "worse case" local SAR levels compared to standard phase relationships. Two different phase configurations for transmit coils were tested. In the all-in-phase case (Fig. 1A) we observed a SAR distribution along the midline whereas in the standard circular excitation (Fig. 1B) the SAR distribution was lateral. The different distribution between the two cases affected also the SAR values for each tissue, with up three-fold SAR changes for CSF and nose.

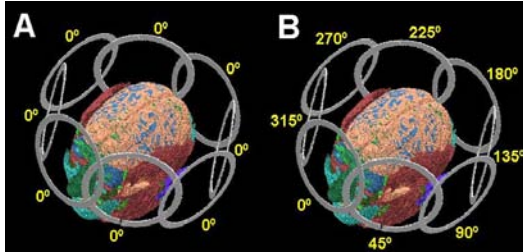


Fig. 1. Eight-channel transmit array coil with high resolution head model (parenchymal tissues visible). Two different phase excitations were tested (A and B). Phases of the sources are reported in yellow.

METHODS SAR distribution was computed by means of FDTD simulations for an eight-channel transmit array coil. A high-resolution ($1 \times 1 \times 1 \text{ mm}^3$) head model based on the anatomical MRI data of an adult male subject was used [1]. 29-tissues were manually/automatically segmented. Eight coils were placed on a cylindrical surface (diameter 250mm) centered around the headmodel (Fig. 1). Each coil was modeled as a ring (diameter 130mm, thickness 10mm, height 1mm) and driven by a 1A current source generator. Two different phase distributions were tested: A) same phase (equal to 0) for all sources (Fig. 1 A); B) circular excitation, i.e. 45° of phase difference between neighbors coils (Fig. 1 B). In both models, whole-head SAR values were normalized to 3W/kg.

	Normalized SAR (W/Kg)			
	Avg.	10g	1g	Max
Model A	3.00	14.86	28.03	61.13
Model B	3.00	11.05	13.07	38.74

Table 1. SAR values for the two different models tested. Values normalized to 3W/Kg for whole-head.

RESULTS In the all-in-phase case (A) the peak 10g-averaged was 1.5 times higher than the guidelines [2] whereas for the circular excitation (B) it was 1.1 times higher (Table 1). Furthermore, the 1g averaged SAR showed a higher than two-fold increase in the local peak in case (A) compared to (B). Finally, the different distribution of SAR in model A (medial) compared to model B (lateral) resulted in three-fold SAR changes for CSF and nose, and in a two-fold SAR change for the nerve (Table 2).

DISCUSSION The results suggest that there is a local increase in SAR in the center of the head only in the case of all-in-phase excitation (A) and not for circular excitation (B) (Fig. 2). Similarly to the case of central brightening effect [3, 4], different configurations and different driving modes of the coils can change the SAR distribution. Furthermore, contrarily to the case of a simple surface coil, the excitation of a single coil, for example the frontal coil, will result in SAR increases even in occipital areas, due to the cross-coupling between all the coils (data not shown). These possible "worse cases" should be taken into consideration when estimating SAR distribution and designing B_1 shimming.

CONCLUSIONS Using FDTD simulations with a high-resolution head model, we show that the transmit array's phase relationship can result in local SAR distribution along the midline (all-in-phase case) or laterally (circular excitation). Furthermore, the SAR values for each tissue can be greatly affected, with up to three-fold SAR changes observed for CSF and nose.

ACKNOWLEDGEMENTS This work was supported by NIH grants R01 EB002459, P41 RR014075, and the MIND institute.

REFERENCES. [1] Angelone et al. ISMRM proceedings 2005. [2]. International Electrotechnical Commission 601-2-33: Geneva. 2002. [3] Ibrahim, T.S., et al., IEEE Trans Biomed Eng. 2005. 52(7): p. 1278-84. [4]. Collins, C.M., et al., J Magn Reson Imaging, 2003. 18(3): p. 383-8.

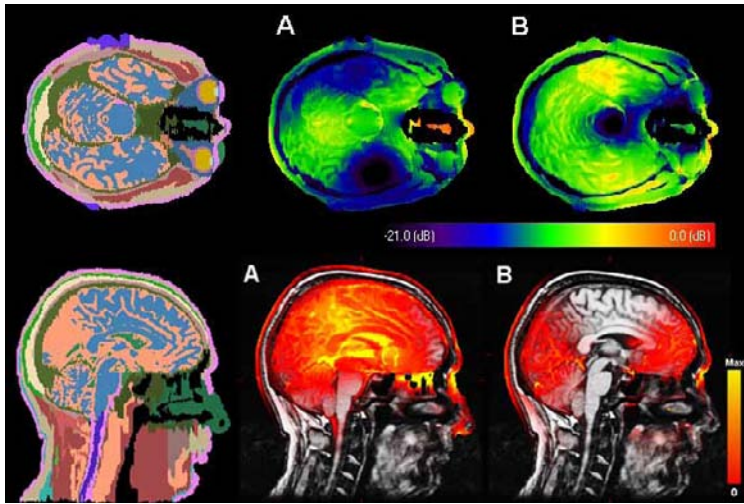


Fig. 2. SAR distribution. (Top) Axial view of SAR values for high resolution head model. The SAR distribution was along the midline (A - all-in-phase case) or lateral (B - circular excitation) $0 \text{ dB} = 0.5 \text{ W/Kg}$. (Bottom) Sagittal view of computed SAR values coregistered with original MRI data used for the headmodel. There was up three-fold SAR changes between the two cases observed for CSF and nose.

Tissue	A	B
CSF	22.0	7.17
Grey Matter	6.4	6.37
White Matter	5.0	4.40
Adipose	0.9	0.72
Bone	0.2	0.18
Conn-Tissue	2.1	2.33
CSF_SA	3.7	2.05
Diploe	2.9	1.82
Dura	3.8	3.86
Ear	1.5	2.86
Epidermis	3.4	3.68
Inner-Table	0.7	0.63
Lens	3.2	3.36
Muscle	1.2	2.10
Nasal-Structures	5.0	1.85
Nerve	5.2	2.68
Orbital-Fat	3.1	2.33
Outer-Table	0.9	0.41
Subcut. Tissue	1.0	1.25
R/C/S	3.4	2.79
SC-Fat/Muscle	2.5	2.83
Soft-Tissue	2.2	1.95
Spinal-Cord	0.4	0.30
Teeth	0.4	0.76
Tongue	1.1	1.67
Vitreous-Humour	4.4	4.10

Table 2. Normalized SAR values (W/kg) averaged over each tissues.